Available online at www.sciencedirect.com
ScienceDirect
Ceramics International 35 (2009) 1321–1325
CERAMICS INTERNATIONAL
www.elsevier.com/locate/ceramint

Effect of diopside addition on sintering and mechanical properties of alumina

Sun Junlong [a,*], Liu Changxia [a], Zhang Xihua [b], Wang baowei [a], Ni Xiuying [a]

[a] Key Laboratory of Advanced Manufacturing and Automation Technology, Ludong University, Yantai 264025, Shandong Province, PR China
[b] School of Materials Science and Engineering, Shandong University, Jinan 250061, Shandong Province, PR China

Received 26 November 2007; received in revised form 21 April 2008; accepted 17 June 2008
Available online 5 August 2008

Abstract

In this paper, diopside was introduced in alumina as a sintering aid and fine structural alumina matrix ceramic materials were fabricated by pressureless sintering. The relative density, hardness, fracture toughness and bending strength of the new fabricated composites were measured. Tribological tests were carried out at a given rotation speed of 160 rpm and in a normal load ranged from 50 to 200 N. The experiment results show that the introduction of diopside can enhance densification rate, which may contribute to the improvement in mechanical properties and result in enhanced wear resistances. The effects of diopside on mechanical properties and microstructures of fine structural alumina matrix ceramic materials were analyzed and discussed.

Keywords: C. Mechanical properties; Alumina; Diopside; Microstructures; Pressureless sintering

1. Introduction

Fine structural ceramic materials are widely applied to measuring instrument, guideway, worktable and high-speed bearing, etc., where high precision durability and long working life are required. Among these fine structural ceramic materials, alumina matrix ceramic material has advantages such as high hardness, good chemical inertness, high wear resistance, low thermal expansion coefficient, low friction coefficient and so on. However, the brittleness of pure alumina limits its potential application as a structural material, and second phases are introduced in alumina matrix to improve its fracture toughness. Excellent mechanical properties are always obtained with an increasing cost owing to expensive second phases [1–5]. Diopside ($MgCa(SiO_3)_2$) has the advantage of low-cost compared to other additives, and it is expected to decrease sintering temperature, reduce porosity and improve mechanical properties. So composites with high ratio of performances versus cost may be obtained, especially for those fine structural ceramics with large dimension.

In this paper, fine structural alumina matrix ceramic materials are fabricated by pressureless sintering in a furnace in N_2 atmosphere. The objective of this work is to investigate effects of diopside on mechanical properties and microstructures of fine structural alumina matrix ceramic materials, as well as to discuss their friction and wear behaviors at a given speed value and different loads. As a result, an approach to produce high performance fine structural ceramics with large dimension and low cost may be found.

2. Experimental procedure

Commercial Al_2O_3 powder of high purity (99.9%) and small grain size (0.5∼1 μm) was used as the starting materials. Diopside ($MgCa(SiO_3)_2$), composed of SiO_2 (55 wt.%), CaO (24 wt.%) and MgO (18 wt.%), was used as an additive. The content of diopside ranged from 1 to 18 vol.% is listed in Table 1. (The suffix in AD_0, AD_1, AD_3, AD_6, AD_{12} and AD_{18} represents the volume content of diopside. For example, AD_0 means the volume content of diopside is zero.)

Firstly, the raw materials were blended with each other according to their proportions and ball milled in an alcohol medium to obtain a homogeneous mixture. Secondly, the slurry was dried in vacuum and screened. Thirdly, green bodies

* Corresponding author. Tel.: +86 15866472132.
E-mail address: sjlthink@126.com (S. Junlong).

0272-8842/$34.00
doi:10.1016/j.ceramint.2008.06.019

Table 1
Compositions and mechanical properties of pressureless sintered alumina matrix ceramics

Specimens	Compositions (vol.%)	Relative density (%)	Hardness (GPa)	Bending strength (MPa)	Fracture toughness (MPa $m^{1/2}$)
AD_0	100% Al_2O_3	88.6 ± 0.5	7.3 ± 2.0	291 ± 25	4.1 ± 0.7
AD_1	99% Al_2O_3 + 1% diopside	94.7 ± 0.2	13.1 ± 1.6	301 ± 21	4.3 ± 0.4
AD_3	97% Al_2O_3 + 3% diopside	97.2 ± 0.3	15.6 ± 1.0	417 ± 14	5.2 ± 0.2
AD_6	94% Al_2O_3 + 6% diopside	97.5 ± 0.3	13.7 ± 1.4	359 ± 15	5.3 ± 0.3
AD_{12}	88% Al_2O_3 + 12% diopside	97.9 ± 0.4	13.5 ± 1.5	330 ± 17	5.0 ± 0.5
AD_{18}	82% Al_2O_3 + 18% diopside	98.3 ± 0.6	12.1 ± 1.8	251 ± 20	4.2 ± 0.5

(50 mm × 50 mm × 50 mm) were shaped using isostatic cold pressing in rubber molds. Lastly, the green bodies were sintered at 1520 °C (heating rate: 20 °C/min) for 140 min in N_2 atmosphere using pressureless sintering.

The sintered bodies were cut into specimens using a slicer and then standard test pieces (3 mm × 4 mm × 36 mm) were ground and polished with diamond paste. Three-point-bending mode was used to measure the bending strength on an electronic universal tensile testing machine (WD-10) with a span of 20 mm at a crosshead speed of 0.5 mm/min. Twelve specimens for each composite were used to measure the bending strength in air at room temperature. Vickers hardness was measured on polished surface with a load of 9.8 N for 5 s with a micro-hardness tester (MH-6). Fracture toughness measurement was performed using indentation method. The indentations on the sample surfaces were generated in a hardness tester (Hv-120), and the formula proposed by Cook and Lawn [6] was used to calculate the final fracture toughness. XRD (D/max-2400) analysis was adopted to identify the phases before and after sintering. Microstructures of the specimens were studied on fracture surfaces and polished surfaces by scanning electron microscopy (HITACHI S-570).

Tribological tests were carried out using a block-on-ring apparatus (MRH-3) under an unlubricated condition, in air, at room temperature, at a given rotation speed of 160 rpm and with varying loads (50, 100, 150 and 200 N). The contact schematic diagram of the frictional couple is shown in Fig. 1. A plain carbon steel ring (HRC 38–45) with outer diameter of 50 mm, inner diameter of 35 mm and thickness of 10 mm, was used as the counterpart. The investigated ceramics were cut into specimens with dimensions of 5 mm × 8 mm × 16 mm. The specimens were ground and polished with diamond paste to an average surface roughness of 0.1 μm. Sliding was performed over a period of 30 min.

The friction coefficient is calculated according to the equation as follows:

$$\mu = \frac{M}{P \cdot R} = \frac{F}{P} \tag{1}$$

where μ is friction coefficient, M is force moment of friction, R is the outer radius of carbon steel ring (25 mm), P refers to the normal load (N) and F to friction force (N). P and F can be directly read from the digital display of the apparatus.

The wear rate is obtained by the following formula:

$$\omega = \frac{V}{L \cdot P} \tag{2}$$

where ω is wear rate ($m^3\ N^{-1}\ m^{-1}$), V is the volume loss of the test specimens (m^3) and L refers to the sliding distance (m).

The volume loss V of the block specimens in Eq. (2) is calculated and determined by the expression [7]:

$$V = \frac{BR^2}{a-b}\left[a\sin^{-1}\frac{a}{2R} + \sqrt{4R^2-a^2} - b\sin^{-1}\frac{b}{2R} - \sqrt{4R^2-b^2}\right] + \frac{2B}{3(a-b)}\left[\left(R^2-\frac{b^2}{4}\right)^{\frac{3}{2}} - \left(R^2-\frac{a^2}{4}\right)^{\frac{3}{2}}\right] \tag{3}$$

where B is the width of the test specimens (m), a and b refer to the dimensions of wear traces on the block specimens, shown in Fig. 2 and measured with a digital-reading microscope (JC-10). The average of three replicate test results is adopted in order to minimize data scattering and decrease the relative error.

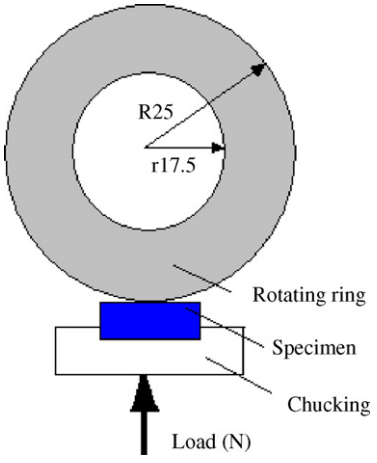

Fig. 1. Contact schematic diagram for the frictional couple.

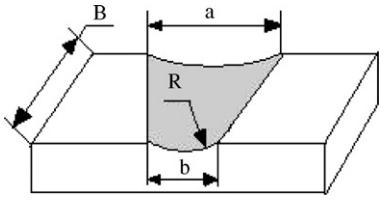

Fig. 2. Schematic diagram of wear traces on the block specimens.

3. Results and discussion

3.1. X-ray diffraction phase analysis

The X-ray diffraction analysis of AD_3 powders before and after sintering at 1520 °C for 140 min, are shown in Fig. 3(a) and (b), respectively. It can be seen from Fig. 3(a) that there exist Al_2O_3, SiO_2 and CaO phases in the ball-milled powders. MgO is not found in Fig. 3(a) for the reason that the content of MgO is too small to be detected by XRD. Fig. 3(b) shows that there exist in AD_3 specimen the phases of Al_2O_3, mullite ($3Al_2O_3{\cdot}2SiO_2$), anorthite CAS_2 ($CaO{\cdot}Al_2O_3{\cdot}2SiO_2$), and CA6 ($CaO{\cdot}6Al_2O_3$). There are no traces of CaO and SiO_2 phases, which may react with alumina, leading to interface reactions and strengthened grain boundaries.

The sintering temperature is 1520 °C, which is higher than the melting point of diopside (1300–1390 °C), diopside will produce liquid phase and the following chemical reactions, yielding mullite, anorthite, and $CaO{\cdot}6Al_2O_3$, may occur during the sintering process:

$$3Al_2O_3 + 2SiO_2 \rightarrow 3Al_2O_3{\cdot}2SiO_2 \quad (4)$$

$$CaO + Al_2O_3 + 2SiO_2 \rightarrow CaO \cdot Al_2O_3{\cdot}2SiO_2 \quad (5)$$

$$6Al_2O_3 + CaO \rightarrow CaO \cdot 6Al_2O_3 \quad (6)$$

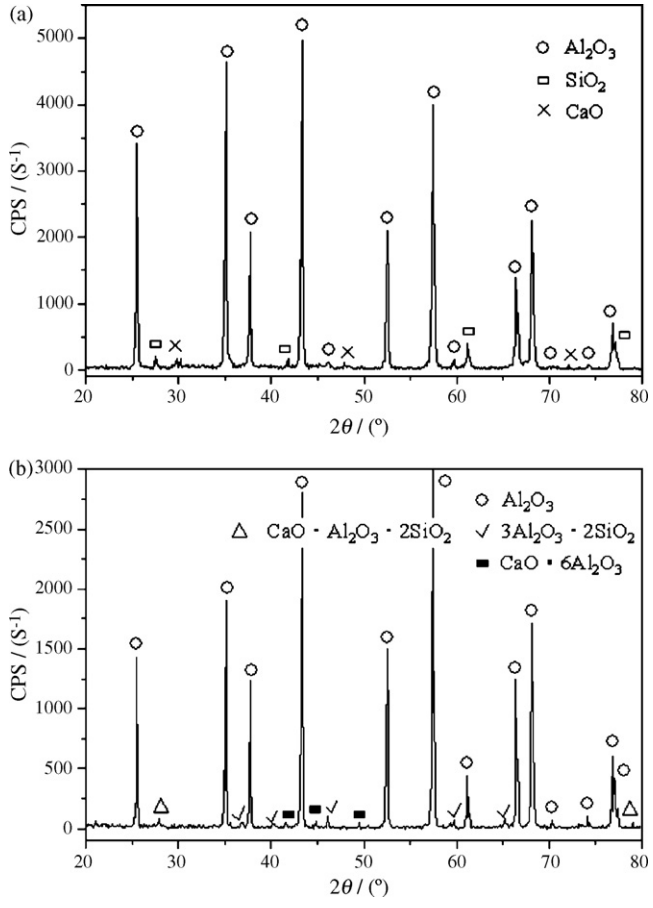

Fig. 3. (a) XRD pattern of AD_3 powder before sintering. (b) XRD pattern of AD_3 specimen sintered at 1520 °C for 140 min.

Based on thermodynamic analysis of the reactions, we can get the following rankings [8]:

$$\Delta G^{\theta}_{T4} < 0, \quad \Delta G^{\theta}_{T5} < 0, \quad \Delta G^{\theta}_{T6} < 0 \quad (7)$$

where ΔG^{θ}_{T4}, ΔG^{θ}_{T5} and ΔG^{θ}_{T6} represent the Gibbs free energy of Eqs. (4)–(6), respectively. XRD analysis shows that mullite, anorthite and $CaO{\cdot}6Al_2O_3$ actually exist in specimen of AD_3 as previously mentioned.

3.2. Mechanical properties

Mechanical properties of composites with different content of diopside are listed in Table 1. As seen from Table 1, hardness of the composites increases with increasing diopside content from 0 to 3 vol.%, and then decreases from 3 to 18 vol.%. Bending strength increases sharply with increasing the amount of diopside before 3 vol.%, at which point it reaches the maximum values of 417 MPa, and then decreases after 3 vol.%. Fracture toughness increases as diopside content is increased from 0 to 6 vol.% and reaches its maximum value of 5.3 MPa $m^{1/2}$, then decreases from 6 to 18 vol.%.

It is obvious that the fabricated fine structural alumina matrix ceramic materials, pressureless sintered at 1520 °C for 140 min in N_2 atmosphere, exhibit significant improvements in mechanical properties. Composite with an addition of 3 vol.% diopside shows excellent mechanical properties, the hardness, bending strength and fracture toughness of the composite reach 15.6 GPa, 417 MPa and 5.2 MPa $m^{1/2}$, respectively.

3.3. Analysis of microstructures

SEM photograph on fracture surface of pure alumina pressureless sintered at 1520 °C for 140 min is shown in Fig. 4(a), and that of AD_3 is shown in Fig. 4(b). It can be seen from Fig. 4(a), grain shape of pure alumina is regular and almost circular. There are pores among incomplete developed alumina grains. The grain boundaries of pure alumina are observable and the fracture mode is mainly intergranular. There are significant microstructural differences among the composites and pure alumina. Evidently, composite with 3 vol.% diopside has a finer grain size compared to pure Al_2O_3, which shows that introduction of diopside may restrain abnormal grain growth of Al_2O_3. It is reported that the existence of magnesia (MgO) in diopside can suppress abnormal grain growth of alumina, promote enhanced densification rate and accelerate the sintering rate [9–11]. As a result, fine and homogeneous microstructures are obtained. It can be clearly seen from Fig. 4(b) that the fracture mode becomes combination of intergranular and transgranular fracture owing to the introduction of diopside. The grain bondings are strengthened when the fracture mode becomes the combination of transgranular fracture and intergranular fracture.

Fig. 5(a) and (b) respectively shows the SEM photomicrographs on polished surface of pure alumina and AD_3 specimen. It can be clearly seen from Fig. 5(a) that there exist apparent pores on the polished surface of pure alumina. Pores, however,

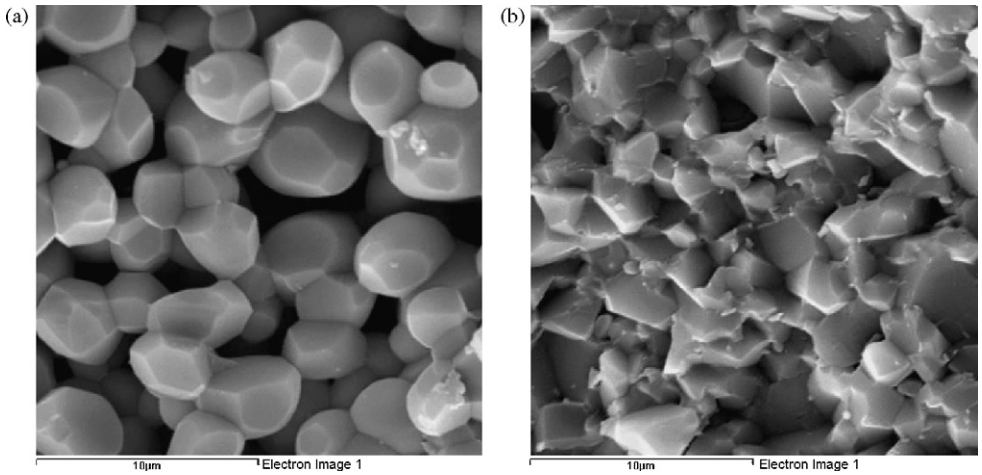

Fig. 4. (a) SEM photomicrograph on fracture surface of pure Al_2O_3 (5000 times). (b) SEM photomicrograph on fracture surface of AD_3 specimen (5000 times).

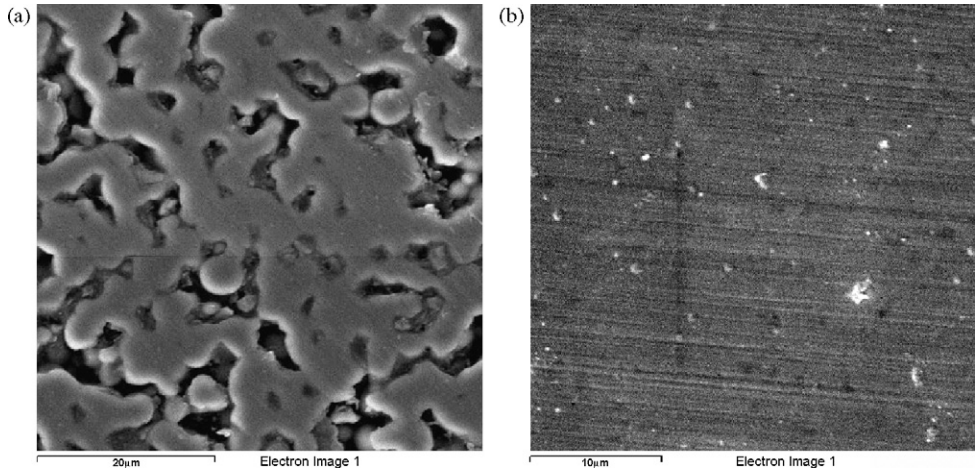

Fig. 5. (a) SEM photomicrograph on polished surface of pure Al_2O_3 (2000 times). (b) SEM photomicrograph on polished surface of AD_3 specimen (3000 times).

on polished surface of AD_3 specimen almost disappear (Fig. 5(b)), making it clear that the introduction of diopside decreases porosities in fine structural alumina matrix ceramic materials.

3.4. Tribological behavior: friction coefficient and wear rate of the composites

The measured friction coefficients of AD_0, AD_3, AD_6 and AD_{12} at different normal loads are shown in Fig. 6. In general, the friction coefficients of specimens increase with the increasing of normal load, and in the range of loads studied in this work, the friction coefficient of composites toughened by diopside are lower than that of pure alumina. As seen from Fig. 6, the friction coefficient of pure alumina is in the range of 0.54–0.70, while that of composites toughened by diopside is in the range of 0.44–0.61. It is indicated that addition of diopside decreases friction coefficient of pressureless sintered fine alumina matrix ceramic composites. Li and Sun [12] have investigated tribological behavior of zirconia-toughened alumina matrix ceramic materials by using a block-on-ring apparatus under an unlubricated condition, in air, at room temperature. Their experimental results showed that the friction coefficient was in the range of 0.73–0.81. Obviously, the friction coefficient of composites investigated in this work is smaller than that of composites toughened by zirconia under similar experimental conditions. It may be owing to the fine and homogeneous microstructures of the new fabricated composites.

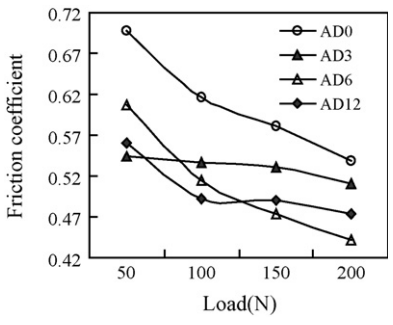

Fig. 6. Friction coefficient of test specimens as a function of normal load.

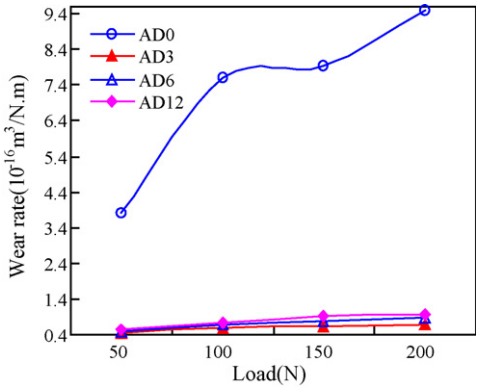

Fig. 7. Wear rate of test specimens as a function of normal load.

The wear rate as a function of normal load for pure alumina (AD_0), AD_3, AD_6 and AD_{12} specimen is shown in Fig. 7. The wear rate increases with the increasing of normal load. There is the increasing of approximately 150% for pure alumina, 64.6% for AD_3, 75.2% for AD_6 and 73.8% for AD_{12}, as the normal load ranges from 50 to 200 N. It is evident that effect of normal load on wear rate of the composites toughened by diopside is slighter than that on wear rate of pure alumina. The highest wear rate of 0.95×10^{-15} m^3/N m was observed for pure alumina at the speed of 160 rpm and load of 200 N, while the highest wear rate of alumina matrix ceramic composites toughened by diopside at the same speed and normal load is 0.97×10^{-16} m^3/N m. Compared to the experimental results obtained by Li and Sun [12] and Pang et al. [13], the wear rate of composites investigated in this work is smaller. It can be seen from Fig. 7 that fine alumina matrix ceramic materials toughened by diopside show low wear rate of magnitude 10^{-16} m^3/N m, smaller than that of pure alumina (10^{-15} m^3/N m). This is mainly due to the different microstructure and porosity. Doğan and Hawk [14] and Basu et al. [15] have reported that mechanical properties and microstructural factors such as grain size and porosity can play a significant role in wear behavior of a polycrystalline alumina ceramic. The improved mechanical properties (Table 1), the fine and homogeneous microstructures (Fig. 3(b)), the decreasing of pores (Fig. 4(b)), all contribute to improved wear resistant of the fabricated composites. The wear rate of AD_3 specimen is lowest (0.42×10^{-16} m^3/N m), and the lowest wear rate is obtained owing to improved mechanical properties, decreasing of pores, as well as fine and homogeneous microstructure of AD_3 specimen.

4. Conclusion

Fine structural alumina matrix ceramic materials are fabricated by pressureless sintering. Introduction of diopside can enhance the densification rate of alumina matrix ceramic materials. Composite with an addition of 3 vol.% diopside shows excellent mechanical properties, including hardness of 15.6 GPa, bending strength of 417 MPa and fracture toughness of 5.2 MPa m$^{1/2}$. The fracture mode of pure Al_2O_3 is mainly intergranular, while that of composites toughened by diopside is a combination of transgranular and intergranular fracture. Furthermore, diopside can decrease porosity and restrain abnormal grain growth, which results in enhanced mechanical properties and improved tribological behaviors. The friction coefficient is effectively decreased and a good wear rate of 10^{-16} m^3/N m is obtained for fine structural alumina matrix ceramic materials toughened by diopside.

Acknowledgements

The work described in this paper is supported by the Specialized Personnel Invitation Rewards of Ludong University (No. LY20074303 and No. LY20074302), the Natural Science Foundation of Shandong Province (No. Y2007F29).

References

[1] S.K.C. Pillai, B. Baron, M.J. Pomeroy, S. Hampshire, Effect of oxide dopants on densification, microstructure and mechanical properties of alumina-silicon carbide nanocomposite ceramics prepared by pressureless sintering, J. Euro. Ceram. Soc. 24 (2004) 3317–3326.
[2] J. Chandradass, M. Balasubramanian, Sol–gel based extrusion of alumina–zirconia fibres, Mater. Sci. Eng. A 408 (1–2) (2005) 165–168.
[3] Wataru Nakao, Masato Ono, Sang-Kee Lee, et al., Critical crack-healing condition for SiC whisker reinforced alumina under stress, J. Euro. Ceram. Soc. 25 (16) (2005) 3649–3655.
[4] Eric Laarz, Mats Carlsson, Benoît Vivien, et al., Colloidal processing of Al_2O_3-based composites reinforced with TiN and TiC particulates, whiskers and nanoparticles, J. Euro. Ceram. Soc. 21 (8) (2001) 1027–1035.
[5] Bo Zhang, Freddy Boey, The phases and the toughening mechanisms in (Y) ZrO_2–Al_2O_3- (Ti, W) C ceramics system, Mater. Lett. 43 (4) (2000) 197–202.
[6] R.F. Cook, B.R. Lawn, A modified indentation toughness technique, J. Am. Ceram. Soc. 66 (11) (1983) 200–201.
[7] Caiqiao Gao, Jiajun Liu, Adhesive Abrasion and Fatigue Wear of Material, Mechanical Industry Press, Peking of China, 1989, pp. 80–243.
[8] D.L. Ye, J.H. Hu, Handbook of The Thermodynamic Data of Inorganic Substances, Metallurgical Industry Press, Peking of China, 2002 pp. 57–1061.
[9] K.A. Berry, M.P. Harmer, Effect of MgO solute on microstructure development in Al_2O_3, J. Am. Ceram. Soc. 69 (2) (1986) 143–149.
[10] S. Baik, J.H. Moon, Effect of magnesium oxide on grain-boundary segregation of calcium during sintering of alumina, J. Am. Ceram. Soc. 74 (4) (1991) 819–822.
[11] S.I. Bae, S. Baik, Critical concentration of MgO for the prevention of abnormal grain growth in alumina, J. Am. Ceram. Soc. 77 (10) (1994) 2499–2504.
[12] D.F. Li, J.L. Sun, Investigation of the tribological behavior of zirconia toughened alumina sliding in air, Surf. Technol. 32 (1) (2003) 19–21 (in Chinese).
[13] Y.X. Pang, Y.J. Quo, H.C. Liu, Study of friction and wear behaviors of Al_2O_3 matrix ceramic in various conditions, Lubrication Eng. 1 (2001) 32–33 (in Chinese).
[14] C.P. Doğan, J.A. Hawk, Role of composition and microstructure in the abrasive wear of high-alumina ceramics, Wear 225–229 (1999) 1050–1058.
[15] Bikramjit Basu, Jozef Vleugels, Omer Van Der Biest, Microstructure–toughness–wear relationship of tetragonal zirconia ceramics, J. Euro. Ceram. Soc. 24 (2004) 2031–2040.